Domains and domain wall interactions near the improper ferroelastic phase transition of KSCN

1993 J. Phys.: Condens. Matter 5 3871

(http://iopscience.iop.org/0953-8984/5/23/014)

J. Phys.: Condens. Matter 5 (1993) 3871–3882. Printed in the UK

Domains and domain wall interactions near the improper ferroelastic phase transition of KSCN

W Schranz and I Rychetsky†
Institut für Experimentalphysik, Universität Wien, A-1090 Wien, Austria

Received 11 November 1992, in final form 8 March 1993

Abstract. In the present paper we study the evolution of the ferroelastic domains and domain wall interactions of KSCN with temperature using a polarizing microscope. The typical lens shape of the ferroelastic domains in KSCN and the change of their shape (i.e. the width and length) with temperature are explained in terms of the dislocation theory for twin boundaries. The interface between the high- and low-symmetry phases was found to be at 45° orientation with respect to the ferroelastic domain walls, in agreement with recent theoretical results.

1. Introduction

In preceding papers we have studied experimentally (Schranz *et al* 1988) and theoretically (Janovec *et al* 1989, Rychetsky 1991, Rychetsky *et al* 1992, Rychetsky and Schranz 1993a, b, Schranz *et al* 1992) the domains and domain walls in the ordered phase of KSCN. The motivation for these studies was the observation of lenticular ferroelastic domains in the ordered phase of KSCN and related crystals. Wedge-shaped twins have been studied previously in indium–thallium alloys (Basinski and Christian 1954). More recently similar lenticular domains have also been found in ferroic crystals, e.g. in $Pb_3(PO_4)_2$ (Torrès *et al* 1982a, b), KH_2PO_4 (Bornarel 1972), Ln_2O_3 (Boulesteix *et al* 1983), $Rb_3H(SeO_4)_2$ (Schranz *et al* 1992), $[N(CH_3)_4]_2\,MnCl_4$ (Fuith *et al* 1990b), and $YBa_2Cu_3O_{7-x}$ (Boulesteix 1989, Snoeck *et al* 1989, Favrot *et al* 1991). In most of these cases the needle or lens shape has been interpreted as a result of the interaction between two domain walls in a so-called triple junction, which is built of two perpendicular domain walls.

In these papers the ferroelastic domain walls are described by the continuum theory of dislocations (Torrès *et al* 1982b, Yamamoto *et al* 1977a) as has been done earlier for the study of ferromagnetic domain walls (Kléman and Schlenker 1972) or the boundaries between mechanical twins (Klassen-Neklyudova 1964, and references therein). In such a description the junction between two perpendicular domain walls is analogous to a partial disclination of wedge type, giving rise to long-range stresses. Two such junctions attract each other and finally they merge to form a needle domain. Around the end of such needle-shaped domains the orientation of the domain wall deviates from the coherent twin plane, which can be described by a distribution of Shockley half-dislocations (Kosevich and Boiko 1971, Bornarel 1972). The inclined boundaries near the tip of isolated and repeated wedge microtwins have been studied in great detail by electron microscopy (Boulesteix *et al* 1983, Yangui *et al* 1982). The shape of thin twins has been extensively studied by Kosevich

† Permanent address: Institute of Physics, Czech Academy of Sciences, Na Slovance 2, 18040 Prague, Czech Republic.

0953-8984/93/233871+12$07.50

and Boiko (1971, and references therein). In the present paper we show the evolution of the ferroelastic domains and the interaction between ferroelastic domain walls at different temperatures near the improper ferroelastic phase transition in KSCN, and describe the observed effects in terms of the dislocation theory.

We have also studied the orientation of the interface between the tetragonal and the orthorhombic phase and compared it with the theoretical results obtained from the phenomenological Landau theory (Rychetsky 1991). A typical etching pattern is observed whose orientation is consistent with recent theoretical results for the orientation of antiphase boundaries in KSCN (Rychetsky and Schranz 1993a). In section 2 we describe briefly the phase transition of KSCN and repeat the basic symmetry relations between the different domain states. The experimental details on the domains and domain walls of KSCN will be presented in section 3 and they will be discussed in section 4.

2. Structure–symmetry relations and phase transition properties of KSCN

In this section we will shortly review the basic properties connected with the order–disorder phase transition in KSCN. KSCN is built of SCN^- dipoles and K^+ ions. In the orthorhombic phase D_{2h}^{11} ($Pbcm$) the SCN^- dipoles form an ordered antiparallel arrangement (Yamamoto *et al* 1987). At $T_c = 142\,°C$ the crystal undergoes an order–disorder phase transition to a tetragonal phase with the space group $D_{4h}^{18}(I4/mcm)$. Above T_c the SCN^- dipoles are head–tail disordered leading on average to the tetragonal structure. Quite recently the temperature dependence of the long-range order parameter η was studied by birefringence measurements (Fuith *et al* 1990a) and described in terms of a compressible pseudospin model (Schranz *et al* 1989a). This model describes the experimental data rather well and shows the importance of the interaction between the strain e and the order parameter η of the type $\eta^2 e$, which determines the temperature dependence of the spontaneous strain e^s in the ordered phase.

The symmetry change $I4/mcm(Z = 1) \rightarrow Pbmc(Z = 2)$, which is accompanied by a doubling of the unit cell, leads to the appearance of two ferroelastic orthorhombic domains and two translational domains. We will denote them as $1_1, 2_1, 1_2$ and 2_2 respectively, where the subscript denotes the translational domain state within the ferroelastic state 1 or 2.

Two ferroelastic domains $1_1, 2_1$ are related by a rotation of $\pi/2$ around the fourfold c axis of the tetragonal parent phase (figure 1). There exist just two perpendicular planes with normals [100] and [010] along which ferroelastic domains can meet coherently (ferroelastic domain wall, FDW). Throughout the whole paper we use the (x, y)-coordinate system which is rotated by $\pi/4$ around the c axis of the crystal with respect to the (x', y')-coordinate system of Schranz *et al* (1989a, b, 1988) and Janovec *et al* (1989). In this coordinate system the spontaneous strain can be represented by a pure shear e_{xy}^s as indicated in figure 1.

Two translational domains, e.g. $1_1, 1_2$, are related by a shift of the tetragonal lattice by the vector $\boldsymbol{x} = (a/\sqrt{2}, 0, c/2)$ (Janovec *et al* 1989), and separated by an antiphase boundary (APB). Here a and c are the lattice parameters of the tetragonal unit cell in the (x', y')-coordinate system. Since the spontaneous deformation is the same in both domains, all orientations of APBs are permissible and equally probable if they are infinitely narrow. For APBs of finite thickness this is not longer true, as has been shown by Rychetsky (1991) and Rychetsky and Schranz (1993a). We will use these results to describe our etch figures obtained for c plates of KSCN.

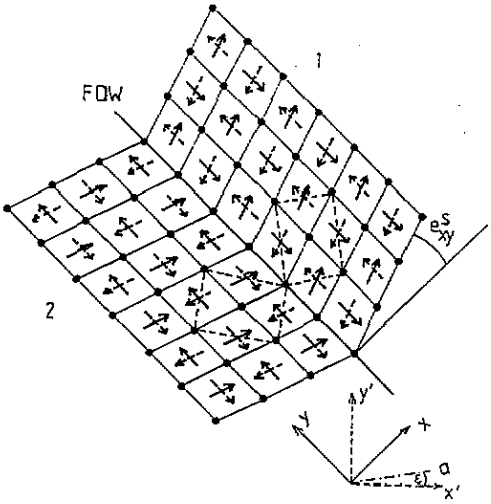

Figure 1. Ferroelastic domain twin with exaggerated spontaneous deformation e^s_{xy}. The broken lines mark the orthorhombic unit cells (a, b) of both domains as previously used (Janovec *et al* 1989). The two domains have been rotated by the angles $\pm\epsilon$ around z to achieve physical contact along the wall.

3. Experimental results

3.1. Ferroelastic domains and domain walls ($1_1/2_1$)

There exist just two planes (100) and (010) along which the ferroelastic domains 1_1 and 2_1 can meet coherently (Sapriel 1975). These planes correspond to the mirror planes lost at the phase transition (Janovec 1989). In contrast to these results no single planar ferroelastic domain wall has been observed in KSCN. The shape of the ferroelastic domains in KSCN, observed as growth twins, mechanical twins and transformation twins, has the form of a lens in all these cases. A typical example is given in figure 2, showing some isolated ferroelastic lenses 1 embedded in the ferroelastic domain 2. The ferroelastic lenses can be characterized by their length L and the width h. At room temperature the ration $h/L = 0.02$ in most cases. h/L changes with temperature, as will be discussed in section 4. The two domain states 1 and 2 can be distinguished in polarized light. The contrast along the ferroelastic wall is due to total refraction.

To obtain a complete picture of the shape of the ferroelastic domains in KSCN, we have cut the crystal in several directions ([100], [010] and [110]) and observed the domains at different temperatures. Figure 3 shows a photomicrograph of an a plate. From this figure one can clearly see the lens shape of the ferroelastic domains elongated along the c direction.

In the following experiment we have observed the temperature behaviour of a single ferroelastic lens of orientation 1 in the matrix 2. To avoid the influence of the interaction between different domains, it was necessary to use isolated lenses. Figure 4 shows the temperature dependences of the length and width of ferroelastic lenses and a comparison with the theoretical results of section 4. After every temperature step we had to wait for about 30 minutes to obtain the equilibrium value of the length and the width of the lenses. We have measured this temperature dependence of L and h several times on different samples and obtained reproducible results (figure 4).

According to figure 4(a) the length of the lenses increases strongly with increasing temperature, resulting in a crossover from the lens shape to planar and 'infinitely extended' FDW. Since the phase transition in KSCN is of first order (Fuith *et al* 1990a), the length does not strictly diverge at T_c (see equation (5) later). Figure 5(a) shows the crossover of the ferroelastic domains from the lens shape (A) to the planar domains (B) near T_c.

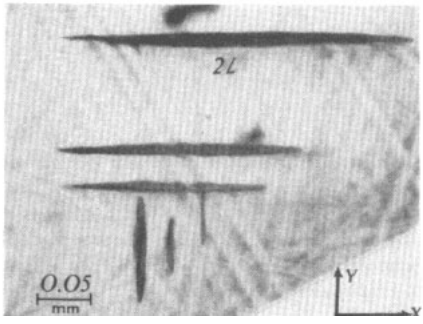

Figure 2. Photomicrograph of a *c* plate of KSCN at room temperature showing the isolated ferroelastic lenses.

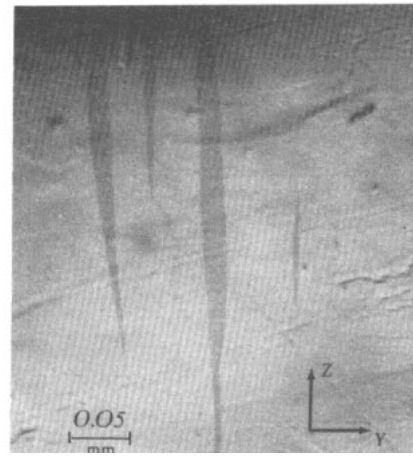

Figure 3. Photomicrograph of an *a* plate. In this projection the lenticular shape of the ferroelastic domains is clearly visible.

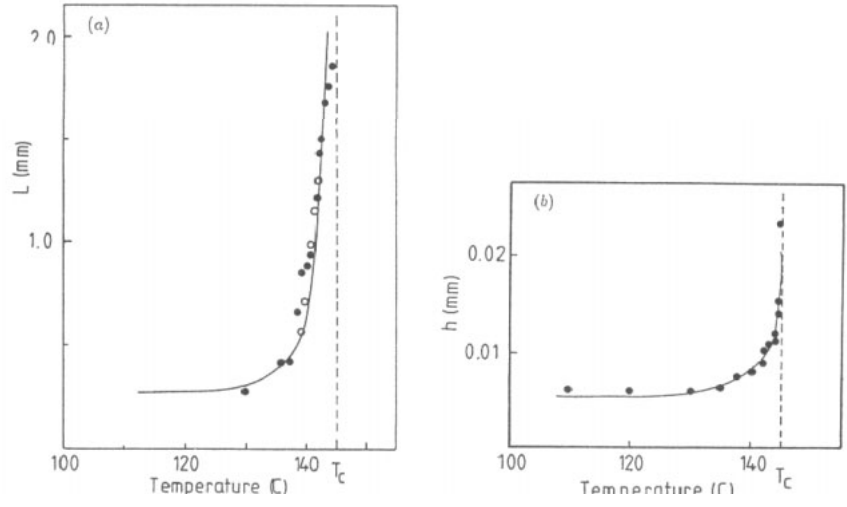

Figure 4. (*a*) Temperature dependence of the length L of ferroelastic lenses: ● experimental data; fit to equation (5) of section 4. (*b*) Temperature dependence of the width h of ferroelastic lenses: ● experimental data; fit to equation (6) of section 4.

The ferroelastic domains merge very near T_c leading to different domain wall intersections (figure 5(*a*) B and figure 5(*b*) +−). Similar intersections of ferroelastic domain walls have been studied experimentally and theoretically by different authors (see e.g., Torrès *et al* 1982a, b, Yamamoto *et al* 1977a, b; for a review see e.g., Salje 1990).

At the end of this section we shall remark on the following observation. Starting with a monodomain sample below T_c, during heating the crystal splits into several ferroelastic

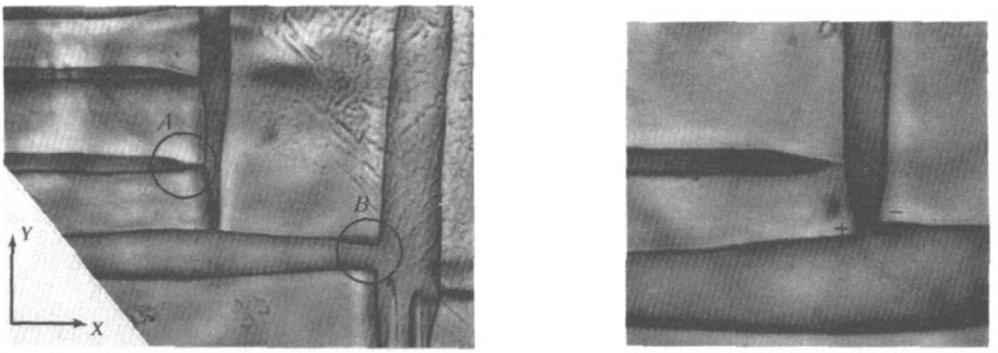

Figure 5. (*a*) Photomicrograph of a *c* plate of KSCN at $T_c - T = 0.05$ K showing the coexistence of lenticular ferroelastic domains (A) with planar domains (region around B); (*b*) photomicrograph of a *c* plate of KSCN at $T_c - T = 0.05$ K showing the interaction between two right-angled domain walls.

domains of typical lens shape, just a few degrees below T_c. With heating, the length of the lenses increases similarly as in figure 4, until they vanish above T_c. This spontaneous appearance of the ferroelastic domains in the ordered phase is (probably) connected with frozen-in static stresses originating from point defects, dislocations, APBs (Rychetsky 1991) or small temperature gradients.

3.2. Translation domains—antiphase boundaries (I_1/I_2)

Because the translation domains do not differ in their macroscopic tensor properties, it is impossible to observe them by optical methods. We tried to visualize them by chemical etching. Figure 6 shows the pattern of a *c* plate of KSCN etched at room temperature. In this figure one can clearly see the ferroelastic walls which form the boundaries of lens-shaped ferroelastic domains. In addition slight etch grooves are visible with preferred orientation along the [110] direction. The neighbouring etching grooves are rotated by $\pi/2$, corresponding to the relative orientation of the adjacent ferroelastic domains.

It is difficult to prove experimentally that this etching pattern really corresponds to the APBs. Nevertheless, in the next section we will show that—according to theoretical results of Rychetsky (1991, Rychetsky and Schranz 1993a)—the APBs in KSCN should be oriented in the direction of the observed etching grooves ([110] or [1$\bar{1}$0]).

3.3. Phase front (D_{4h}/D_{2h})

Since the phase transition is accompanied by a change from the tetragonal to the orthorhombic crystal system, the phase front can be easily visualized between crossed polarizers. Figure 7 shows an example of a phase front, with normals oriented along the [110] direction and perpendicular to it.

To accommodate the high- and low-temperature structures a large number of small orthorhombic domains is formed at the border of the two phases. In the next section we will explain the orientation of the interface using the results of Rychetsky (1991, Rychetsky and Schranz 1993a).

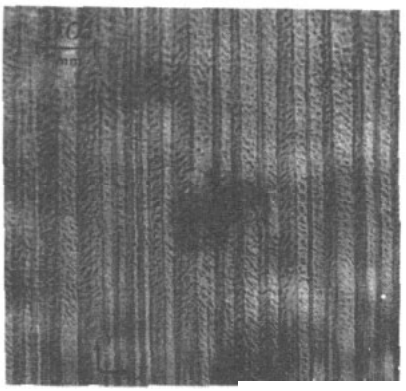

Figure 6. Photomicrograph of a c plate of KSCN etched at room temperature. The etching pattern has a preferred orientation of 45° with respect to the ferroelastic domain walls.

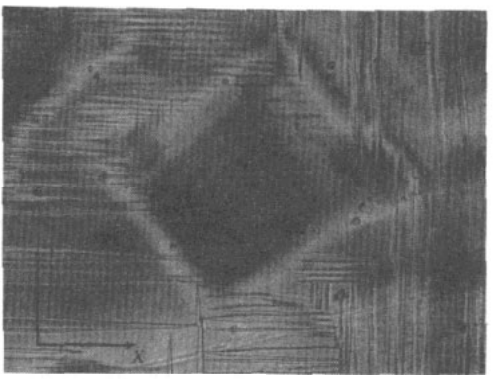

Figure 7. Photomicrograph of a c plate of KSCN showing the interface between the tetragonal parent phase and the orthorhombic low-symmetry phase. The interface is oriented at 45° with respect to the ferroelastic domain walls.

4. Discussion

In this section we shall discuss our experimental results on ferroelastic domains and domain walls, using the well known dislocation theory of FDWs (Kleman and Schlenker 1972, Kosevich and Boiko 1971). The etching pattern as well as the phase front observations will be discussed in terms of the phenomenological Landau theory (Rychetsky 1991, Rychetsky and Schranz 1993a).

4.1. Ferroelastic domains and domain walls

The phase transition in KSCN is driven by a two-component order parameter (η_1, η_2) (Schranz *et al* 1989b). Due to the appearance of the spontaneous order parameter $(\eta_s, 0)$, a spontaneous strain is induced in the orthorhombic phase. In our coordinate system the spontaneous strain can be represented by a pure shear e^s_{xy} in domain 1 and $-e^s_{xy}$ in domain 2. Using the compressible pseudospin model (Schranz *et al* 1989a) for the description of the phase transition in KSCN, the relations

$$e^s_{xy} = k_{xy}\eta_s^2 \tag{1a}$$

$$\eta_s = \tanh[(T_0/T)(\eta_s + A\eta_s^3)] \tag{1b}$$

have been found.

From the fit of equations (1a) and (1b) to the experimental data (Yamamoto *et al* 1987) k_{xy} is determined as $k_{xy} = 0.001\,35$. According to birefringence measurements (Fuith *et al* 1990a) η_s^2 varies from 0.25 at T_c to 0.9 at room temperature, and consequently e^s_{xy} varies from 3.38×10^{-4} to 1.2×10^{-3}.

In the continuum theory of dislocations, a coherent domain wall of zero thickness can be represented by a continuous distribution of dislocations (Kleman and Schlenker 1972). It is important to note that these edge dislocations do not produce any stress field as expected for a coherent planar domain wall.

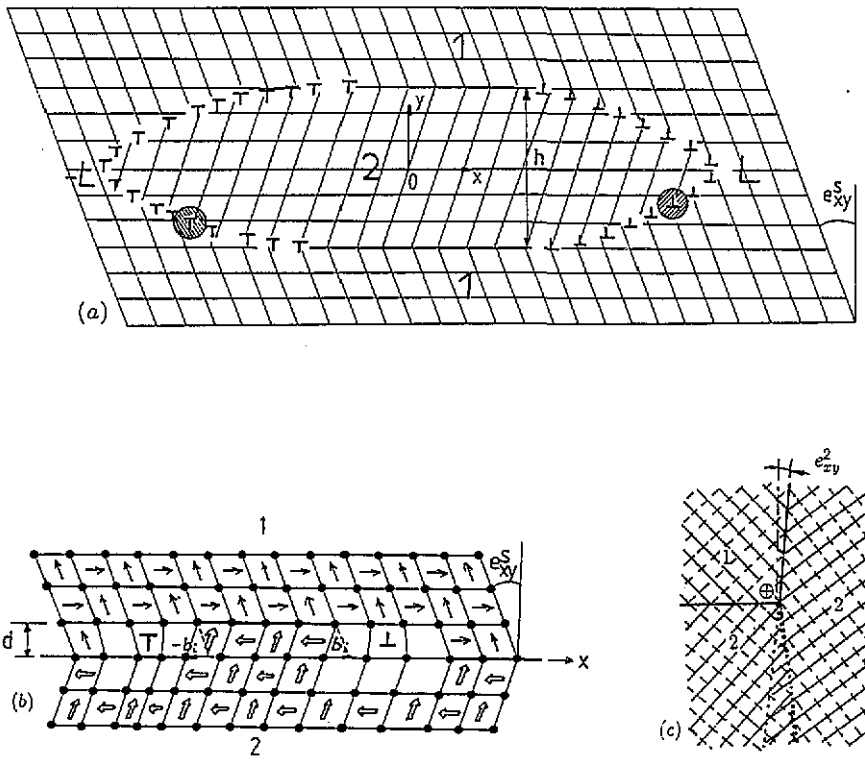

Figure 8. (*a*) Schematic representation of the arrangement of dislocations appearing at the ends of a ferroelastic lens. (*b*) Sketch of a Shockley half-dislocation (shaded circle in (*a*)) of the FDW. The Burgers vector is given by $b_i = 2d \tan e^s_{xy} \simeq 2de^s_{xy}$. Around the dislocation the lattice is distorted as is the orientation of the SCN molecules. In these distorted parts we have omitted the SCN molecules. (*c*) Schematic representation of two wedge disclinations of opposite sign which appear near the junction of two almost perpendicular ($90° \pm e^s_{xy}$) domain walls.

Any deviation of the ferroelastic domain wall from the coherent orientation (in our case these are the (100) and (010) planes) leads to the appearance of new dislocations, which produce long-range stresses. Especially near domain tips, where the wall cannot be in coherent orientation, the wall can be represented by a distribution of Shockley half-dislocations (Bornarel 1972) with Burgers vectors $b_m \simeq 2w_m e^s_{xy}$ (figures 8(*a*), (*b*)). Here w_m is a mean lateral step displacement of the wall, caused by the Shockley half dislocation of a mean Burgers vector b_m (figure 8(*b*)).

Kosevich and Boiko (1971) have studied the equilibrium shape of such an assembly of twinning dislocations for mechanical twins. We will apply this concept for the description of our lens-shaped ferroelastic domains. A thin lens-shaped domain (LSD) (figure 8(*a*)) with $h/L < 1$ is in equilibrium if all the forces acting on each dislocation are equal to zero. These forces are

(a) forces of elastic origin (Peach–Koehler forces)—which take into account the inhomogeneous elastic fields $\sigma^e(x)$ created by the external loads or by impurities, dislocations, etc present in the crystal—which generally support the creation of the domain and

(b) forces of inelastic origin, the surface tension force $S_s(x)$ and the Peierls–Nabarro

force $S_0 \propto \exp(-1/b_m)$ (Nabarro 1967), which hinder the creation of the domain.

The equilibrium condition of a dislocation a the point x can be written as (Kosevich and Boiko 1971)

$$\int_{-L}^{+L} \rho(\xi)/(\xi - x)\mathrm{d}\xi = (1/\mu b)[\sigma^e(x) - S_s(x) - S_0]. \tag{2}$$

Here only the component of the force acting in the direction of the Burgers vector b is taken into account, because the dislocations can move easily only in this direction. $\rho(\xi)$ is the density of twinning dislocations which appear due to the deviation of the domain wall from the coherent orientation and μ is the Lamé coefficient in the isotropic approximation.

Equation (2) determines the shape (i.e. length L and thickness $h(x)$ of an LSD). If the length L of the LSD is very large, it can be approximated by the equation (Kosevich and Boiko 1971)

$$\Phi_0/L = S_0 + M/\sqrt{L} \tag{3}$$

where $\Phi_0 = \int \sigma(x)\mathrm{d}x$ is the integral force of type (a) above and $M \simeq \sqrt{\epsilon} S_s^0$ is due to the surface tension force $S_s(x)$ which differs from zero only in a small neighbourhood ϵ near the end of the twin. From estimations ϵ has been found to be $\sim 10^{-6}$–10^{-5} cm. In our experiments L varies from 10^{-2} to 1 cm. To describe the variation of the length L with temperature, we can neglect the contribution from the surface tension force. Using the explicit form for the Peierls–Nabarro force S_0, equation (3) reads

$$L = \Phi_0/S_0 = \Phi_0[(1 - \nu)/2\mu]\exp(4\pi A_m/b_m) \tag{4}$$

where ν is the Poisson ratio and A_m is a constant determined by the width of the twinning dislocations.

Inserting the spontaneous strain of equation (1) into equation (4), we find that the length L increases exponentially with temperature:

$$L \propto \exp(2\pi A_m/w_m k_{xy}\eta_s^2). \tag{5}$$

Figure 4 shows the good agreement between equation (5) and the experimental results.

At this point we shall make some remarks on the role of the elastic force Φ_0. This force can originate from symmetry-breaking point defects, dislocations or small temperature gradients, etc, always existing in a real crystal. Calculations for different types of defect in the frame of Levanyuk's theory (Levanyuk and Sigov 1988) give a weak temperature dependence of the integrated force in comparison to the exponential one originating from the Peierls–Naborro force and we have put it constant in equation (5).

The thickness h of the LSD can be written as (Kosevich and Boiko 1971)

$$h \simeq \ln L \simeq \text{constant}/\eta_s{}^2(T). \tag{6}$$

A strong increase of the width h of the ferroelastic lenses consistent with equation (6) has been indeed observed near T_c (figure 4(*b*)).

According to equation (5), the length L of the lenses increases exponentially with decreasing η_s and diverges at T_c for a second-order phase transition. Consequently perpendicular lenses touch each other at a temperature very near T_c (figure 5(*a*), A) and finally they merge (figures 5(*a*), B and 5 (*b*)). The resulting junctions which are built by the

intersection of two perpendicular domain walls (figure 5(*b*) + and −) can be represented by wedge-type disclinations of different sign (figure 8(*c*)). Two wedge disclinations of opposite sign (e.g. figure 5(*b*) + and −, figure 8(*c*)) attract each other by a force which in the approximation of an isotropic medium is given by (Kroupa and Lejcek 1972)

$$F_r = -[2\mu(e^s_{xy})^2/\pi(1-\nu)]r\ln(R/r) \tag{7}$$

where r is the distance between the junctions and R defines the core of the dislocation. This force between two right-angled domain walls increases with decreasing r and can be strongly temperature dependent through the temperature dependence of the elastic constant μ and the spontaneous strain e^s_{xy}. For a second-order phase transition F_r goes to zero continuously as $T \to T_c$. It jumps to zero at T_c for a phase transition of first order. This explains the crossover from lenses to rectangles with $T \to T_c$ which has been frequently observed for KSCN. Equation (7) can be used to explain at least qualitatively the difference between ferroelastic domains near proper and improper ferroelastic phase transitions as is observed in experiments. Near proper ferroelastic phase transitions of second order the FDWs are usually planar and 'infinitely' extended (e.g. in $CsLiSO_4$ (Pietrasko *et al* 1981) and $CsHSO_4$ (Ozaki *et al* 1982)), whereas near improper ferroelastic transitions they often form needle-shaped tips (e.g. in $Pb_3(PO_4)_2$, $Rb_3H(SeO_4)_2$ and GMO) or lenses (KSCN, RbSCN, etc). Using equation (7) this difference can be qualitatively explained by the value of the force F_r between right-angled domain walls. Due to the softening of the transverse elastic constant $\mu \to 0$ ($T \to T_c$) at proper ferroelastic phase transitions this force F_r is orders of magnitude smaller than improper ferroelastic phase transitions very near T_c where the domains are usually observed (table 1).

Table 1. Typical values for the attractive force between right-angled domain walls for proper and improper ferroelastic phase transitions of first and second order.

	$\mu(e^s_{xy})^2$	$\mu(e^s_{xy})^2$(N m^{-2}) at $T - T_c = 0.01$ K
Proper ferroelastic second-order phase transition $LiCsSO_4$ (Anistratov *et al* 1983)	$2 \times 10^3(T_c - T)^2$	10^{-1}
Improper ferroelastic extrapolated to second-order phase transition $Pb_3(PO_4)_2$	$5 \times 10^4(T_c^* - T)$	5×10^2
Improper ferroelastic first-order phase transition $Pb_3(PO_4)_2$ (Wood *et al* 1980)	$5 \times 10^4(T_c - T)$	6×10^5
Improper ferroelastic first-order phase transition KSCN	$10^7\eta_s^2(T)$	10^3

Table 1 gives the values of $F_r \propto \mu(e^s_{xy})^2$ for different crystals exhibiting proper and improper ferroelastic phase transitions of first and second order. Comparing these values of F_r, the planar shape of the domain walls observed, e.g., in $CsLiSO_4$ (proper ferroelastic, Pietrasko *et al* 1981) as well as their lens shape which was observed in KSCN (improper ferroelastic) appears plausible.

It should be stressed that the equation (7) used in the above analysis is exact only for an isotropic medium. Nevertheless in the anisotropic case a similar formula holds, at least near proper ferroelastic phase transitions from tetragonal to orthorhombic (e.g. KDP) and

from orthorhombic to monoclinic (e.g. $CsLiSO_4$). In these cases the Lamé coefficient μ in equation (7) is replaced by the corresponding shear elastic constant C_{66} which approaches zero at T_c (Schranz 1993).

4.2. Translation domains—antiphase boundaries (l_1/l_2)

The APB connects two domains e.g. $l_1 = (\eta_s, 0)$ and $l_2 = (-\eta_s, 0)$ with the same deformation on both sides of the wall. In the case of an infinitely narrow APB no restriction is put on the APB orientation. i.e. any orientation is equally probable. This has been clearly demonstrated by electron microscopic studies (Boulesteix 1984). In some cases, however, the APBs may have a finite thickness. An example is $Gd_2(MoO_4)_3$. Electron microscopic studies revealed a thickness for the APB of 30–70 Å which is about 3–7 lattice constants (Yamamoto *et al* 1977b). Barkley and Jeitschko (1973) have shown experimentally that a preferred orientation of the APB which changes strongly with temperature exists in $Gd_2(MoO_4)_3$. APBs of finite thickness have been quite recently studied theoretically by Rychetsky (1991, Rychetsky and Schranz 1993a). In this model the angular dependence of the APB orientation is a consequence of the compatibility condition for the strain tensor. For a special set of parameters the observed temperature dependence of the APB in $Gd_2(MoO_4)_2$ was reproduced (Rychetsky 1991). For another set of parameters one can find that the orientation of the APB is locked in crystallographic orientations. This situation seems to appear in KSCN. After the determination of the parameters in the free energy expansion for KSCN we arrived at the following result (Rychetsky and Schranz 1993a, b): two minima of the APB free energy are symmetrically distributed around $\Theta = 45°$. The APBs are stressed in any orientation with maximum stress at $\Theta = -45°$. The two minima of the domain wall stress are symmetrically distributed around $\Theta = +45°$, implying that the orientation of an APB in KSCN is locked in the crystallographic orientation and does not change with temperature. These theoretical results for the orientation of APBs in KSCN are quite consistent with our observations on etched c plates of KSCN (figure 6). In figure 6 one can see etching grooves oriented mainly at 45° with respect to the orientation of FDWs. However, more direct investigations are necessary to clarify the origin of the observed etch pattern.

4.3. Phase front (D_{4h}/D_{2h})

In the theory of Boulesteix (Boulesteix *et al* 1986, Wadhawan and Boulesteix 1992) the orientation of permissible (strain-free) interfaces is calculated with the assumption that the crystal volume is conserved during the phase transition. In many crystals this theory was found to be in agreement with the observations (Boulesteix *et al* 1986). For KSCN the equation of the permissible planes $2e^s_{xy}xy = 0$ determines the orientations of the interface with normals along [100] and [010] directions. However, according to figure 7 the observed interface in KSCN is oriented in the [110] direction and perpendicular to it. Thus, KSCN seems to be an interesting case, where the change in the volume at the phase transition plays an important role for the orientation of the interface. Removing the assumption of constant volume we can describe the orientation of the interface in a similar way to the orientation of APBs of finite thickness (Rychetsky 1991, Rychetsky and Schranz 1993a). Since the centre of the APB ($\eta_1 = 0, \eta_2 = 0$) has the same structure as the high-temperature phase of KSCN we can directly apply the results obtained for the orientation of APBs of finite thickness (figure 3(c) of Rychetsky 1991). As for the orientation of APBs we obtain 45° for the orientation of the phase front (D_{4h}/D_{2h}) of KSCN in perfect agreement with the observations (figure 7). As for the APBs the phase front is stressed and this stress can be released by the appearance of a large number of small ferroelastic domains (figure 7).

5. Summary

In the present paper we have shown the experimental results concerning the ferroelastic domains and domain walls, etching pattern and phase front orientations observed near the improper ferroelastic phase transition in KSCN using a polarizing microscope. Applying the dislocation theory for thin twins we have described the shape as well as the change of shape (i.e. length and width) of the ferroelastic lenses with temperature. We have also studied the interactions between right-angled ferroelastic domain walls forming wedge disclinations, near T_c. Due to the softening of the shear modulus near proper ferroelastic phase transitions this interaction is smaller by orders of magnitude near T_c than for improper ferroelastic phase transitions. This fact can be used to explain at least qualitatively the different domain pattern observed near proper and improper ferroelastic phase transitions.

The orientation of the interface between the paraelastic and ferroelastic phases was observed in [110] and [1$\bar{1}$0] directions, i.e. inclined by 45° with respect to the ferroelastic domain walls. The difference of this orientation from the [100] and [010] directions which are obtained from the theory of Boulesteix *et al* (1986) indicates that the finite change of the crystal volume plays an important role in the orientation of the interface. A discontinuous volume change of 1.5% has been reported (Shinoda *et al* 1960), consistent with the first-order character of the phase transition. Taking into account this volume change, the orientation of the interface can be described by a phenomenological model which was also used to describe the APBs in KSCN. The calculated orientations are in perfect agreement with the experimental observations.

A typical etching pattern oriented mainly at 45° with respect to the FDWs was found. This direction agrees very well with recent calculations for the orientation of APBs in KSCN. However, a more direct investigation is necessary to clarify whether the etching pattern originates from the presence of APBs or from other types of crystal defect.

Acknowledgments

The present work was performed under project P 8285 of the Österreichischen Fonds zur Förderung der wissenschaftlichen Forschung. One of the authors (IR) is grateful for financial support from the Österreichischen Bundesministerium für Wissenschaft und Forschung.

References

Anistratov A T, Zamkov A V, Kot L A, Stolovitskaya I N and Shabanova L A 1983 *Ferroelectrics* **48** 103
Barkley J R and Jeitschko W 1973 *J. Appl. Phys.* **44** 938
Basinski Z S and Christian J W 1954 *Acta Metall.* **2** 101
Bornarel J 1972 *J. Appl. Phys.* **43** 845
Boulesteix C 1984 *Phys. Status Solidi* a **86** 11
—— 1989 *Phase Transitions* **14** 41
Boulesteix C, Yangui B, Ben Salem M, Manolikas C and Amelinckx S 1986 *J. Physique* **47** 461
Boulesteix C, Yangui B, Nihoul G and Bourret A 1983 *J. Microsc.* **129** 315
Favrot D, Dechamps M and Revolevschi A 1991 *Phil. Mag. Lett.* **64** 147
Fuith A and Kroupa J 1990a *J. Phys. Condens. Matter* **2** 2355
Fuith A, Schranz W, Warhanek H, Kroupa J and Lhotska V 1990b *Phase Transitions* **27** 15
Janovec V, Schranz W, Warhanek H and Zikmund Z 1989 *Ferroelectrics* **98** 171
Klassen-Neklyudova M V 1964 *Mechanical Twinning of Crystals* (New York: Consultants Bureau)
Kleman M and Schlenker M 1972 *J. Appl. Phys.* **43** 3184
Kosevich A M and Boiko V S 1971 *Sov. Phys.–Usp.* **14** 286

Kroupa F and Lejcek L 1972 *Phys. Status Solidi* b **51** K121
Levanyuk A P and Sigov A S 1988 *Phase Transitions* **11** 91
Nabarro F R N 1967 *Theory of Crystal Dislocations (Int. Ser. Monographs on Physics)* (Oxford: Clarendon)
Ozaki T, Itoh K and Nakamura E 1982 *J. Phys. Soc. Japan* **51** 213
Pietrasko A, Tomaszewski P E and Lukasziewicz K 1981 *Phase Transitions* **2** 141
Roucau C, Tanaka M, Torres J and Ayroles R 1979 *J. Mirror. Spech. Electro.* **4** 603
Rychetsky I 1991 *J. Phys.: Condens. Matter* **3** 7117
Rychetsky I and Schranz W 1993a *J. Phys.: Condens. Matter* **5** 1455
—— 1993b to be published
Rychetsky I, Schranz W and Zielinski P 1992 *Ferroelectrics* **126** 383
Salje E K H 1990 *Phase Transitions in Ferroelastic and Co-elastic Crystals* (Cambridge: Cambridge University Press)
Sapriel J 1975 *Phys. Rev.* B **12** 11, 5128
Schranz W 1993 to be published
Schranz W, Rychetsky I and Warhanek H 1992 to be published
Schranz W, Streuselberger T, Fuith A, Warhanek H and Götzinger M 1988 *Ferroelectrics* **88** 139
Schranz W, Warhanek H, Blinc R and Zeks B 1989a *Phys. Rev.* B **40** 714
Schranz W, Warhanek H and Zielinski P 1989b *J. Phys.: Condens. Matter* **1** 1141
Shinoda T, Suga H and Seki S 1960 *Bull. Chem. Soc. Japan* **33** 1314
Snoeck E, Casanove M J, Baules P and Roucau C 1989 *Ferroelectrics* **97** 181
Torres J, Roucau C and Ayroles R 1982a *Phys. Status Solidi* a **70** 659
—— 1982b *Phys. Status Solidi* a **70** 193
Wadhawan V K and Boulesteix C 1992 *Key Eng. Mater.* **68** 43
Wood I G, Wadhawan V K and Glazer A M 1980 *J. Phys. C: Solid State Phys.* **13** 5155
Yamamoto N, Yagi K and Honjo G 1977a *Phys. Status Solidi* a **42** 257
—— 1977b *Phys. Status Solidi* a **44** 147
Yamamoto S, Sakuno M and Shinnaka Y 1987 *J. Phys. Soc. Japan* **56** 4393
Yangui B, Boulesteix C, Bourret A, Nihoul G and Schiffmacher G 1982 *Phil. Mag.* A **45** 443